Parameter analysis of a practical lithium- and sodium-air electric vehicle battery

E. Peled [a,*], D. Golodnitsky [b], H. Mazor [a], M. Goor [a], S. Avshalomov [a]

[a] *School of Chemistry, Tel Aviv University, Tel Aviv 69978, Israel*
[b] *Wolfson Applied Materials Research Center, Tel Aviv University, Tel Aviv 69978, Israel*

ARTICLE INFO

ABSTRACT

For electric vehicles (EV) having a 500 km range between charges, there is a need to develop smaller and lower-cost batteries. Lithium-air has the potential to deliver a step change in the specific energy of rechargeable lithium batteries. In order to develop a practical, safe, smaller and lower-cost lithium and sodium-air rechargeable EV battery it is necessary to eliminate the formation of dendritic deposits (on charge), increase the current density up to $100\,mA\,cm^{-2}$ (or reducing cell DC resistance to less than $10\,\Omega\,cm^2$) and change the oxygen-discharge product from peroxide to oxide. We suggest here a novel concept, namely to replace the metallic lithium anode by liquid sodium and to operate the sodium–oxygen cell above the sodium melting point (97.8 °C). In this report we studied the deposition–dissolution process of sodium in polymer electrolytes at 105 °C and we present, for the first time, preliminary results that demonstrate the feasibility of running a liquid-sodium–oxygen cell with polymer electrolytes at above 100 °C.

© 2010 Elsevier B.V. All rights reserved.

1. Introduction

The state-of-the-art lithium-ion batteries are considered to be the best rechargeable batteries on the market. They consist of a graphitic-carbon anode, a liquid electrolyte comprising lithium salts dissolved in organic solvents, a microporous-polymer separator and a lithium-intercalated transition-metal-oxide positive electrode. Their theoretical specific energy is about $400\text{–}500\,Wh\,g^{-1}$. For many applications, including electrical-energy storage for renewable sources such as solar and wind and for transportation, there is a need to develop smaller and lower-cost batteries. This requires the development of new cell chemistries. Lithium-air has the potential to deliver a step change in the specific energy of rechargeable lithium batteries [1–7]. The theoretical specific energy of the Li–O_2 couple is $5200\,Wh\,kg^{-1}$, including the weight of oxygen and assuming Li_2O as the discharge product. However, the cathodic discharge products are found to be lithium peroxide and lithium superoxide [1–7]; for peroxide, the cell provides a specific energy of $3600\,Wh\,kg^{-1}$ which is eight times that of state-of-the-art lithium-ion cells. Its open-circuit voltage (OCV) is 3.1 V. In contrast to the lithium-ion cell, the rechargeable lithium-air cell has a metallic-lithium anode. In all lithium (as well as in other alkali and alkaline-earth) nonaqueous batteries, the anode is covered by a thin film called a solid electrolyte interphase (SEI) [9–11]. As a result, on charge, lithium deposits through the SEI in the form of lithium dendrites and mossy (sponge) lithium. This raises safety issues, including thermal instability and the formation of internal short-circuits by the lithium dendrites. For these reasons, efforts to develop rechargeable lithium–metal batteries have failed, and today only rechargeable lithium-ion batteries that do not contain metallic lithium are in use.

The lithium-air cell has several other disadvantages: up to now, the power obtained is very low – about $0.1\text{–}1\,mA\,cm^{-2}$ – and the oxygen-discharge products – lithium peroxide and lithium superoxide [7] – are very reactive toward the electrolyte solvents and toward the environment. In addition, they are electrically-insulating materials, thus a large area of carbon substrate is required to accommodate the solid peroxide at a thickness lower than the tunneling range of electrons (that is, the thickness of the lithium-peroxide layer on the carbon matrix must be less than about 25 Å).

In order to develop a practical, safe, smaller and lower-cost rechargeable battery for the applications listed above, it is necessary to eliminate the formation of spongy and dendritic lithium deposits (on charge), to increase the current density by one or preferably two orders of magnitude, up to $100\,mA\,cm^{-2}$ [8] (or reducing cell DC resistance to less then $10\,\Omega\,cm^2$) and change the oxygen-discharge product from peroxide to oxide.

We suggest here a novel concept, namely to replace the metallic lithium anode by liquid sodium and to operate the sodium–oxygen cell above the sodium melting point (97.8 °C). The sodium-air battery could enable the development of a new generation of high-specific-energy rechargeable batteries. In this report we present preliminary results that demonstrate

* Corresponding author. Tel.: +972 3 640 8206; fax: +972 3 641 4126.
E-mail address: peled@tau.ac.il (E. Peled).
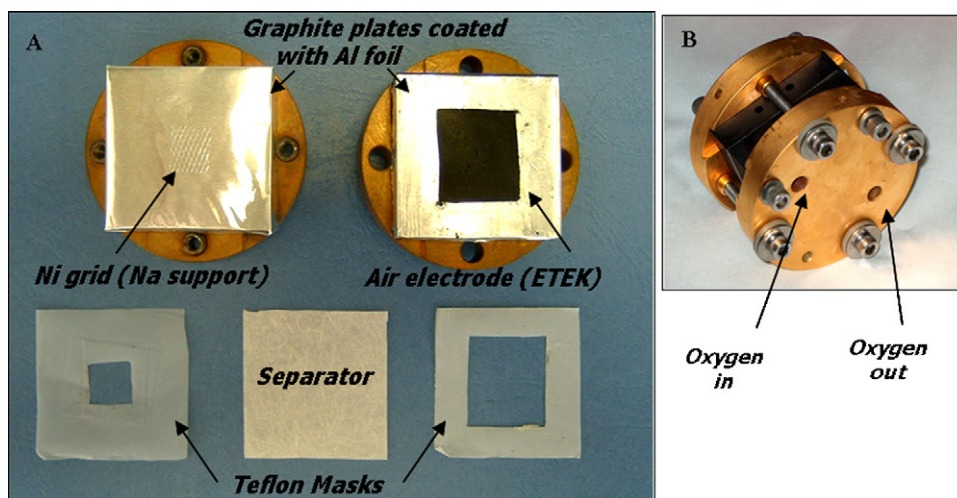
Fig. 1. The basic components (a) and assembled-cell (b) photographs of single-cell sodium/air fuel-cell type hardware.

the feasibility of running a liquid-sodium–oxygen cell at above 100 °C.

2. Experimental

Two types of hardware setups were used. The first (Fig. 1) was similar to the fuel-cell hardware used in our laboratory for DMFC tests described elsewhere [12]; a photograph of it is shown in Fig. 1b. It consists of copper end plates, graphite plates covered with aluminum foil with two holes which enable oxygen flow through the carbon cloth of the ETEK air electrode, a sodium electrode and an ETEK air electrode with a film of electrolyte between them. The basic components of the cell are shown in Fig. 1a. A 360 μm-thick E-TEK electrode (supplied by E-TEK, Somerset, NJ 088730, USA) with 0.3 mg Pt cm^{-2} (10%Pt-supported XC72) coated with 4–5 mg Na_2CO_3 cm^{-2} was used as the air electrode of the Na/air cell. In order to improve electrolyte/electrode contact, 0.1–3 mg cm^{-2} of sodium electrolyte was cast on the air electrode (similar to the Nafion coating of the air electrode in PEM fuel cells). In order to enable homogeneous coating of the electrode by the electrolyte, a surface-active agent, Triton X-100 was added to the slurry. The anode was a 600 μm-thick Na foil of area 1 cm^2. The 150 μm-thick glass separator was saturated with the electrolyte which contained 0.1 M calix[6]pyrrole (CP), 1 M sodium perchlorate (Merck Ltd.) and 1% (w/w) high-surface-area Al_2O_3 powder (Degussa Ltd.) dispersed in polyethylene glycol dimethyl ether (PEGDME 2000 Merck Ltd.)/propylene carbonate (Fluka) (90:10, by volume). All solutions were prepared from analytical-grade chemicals and the electrolyte was dried at 100 °C prior to the saturation of the separator. As the transference number of sodium is expected to be low, we added the anion trap calix[6]pyrrole (CP) in order to increase it. This was shown, by our group, to be successful in the case of lithium [13]. In addition, such an anion trap may complex the O^{2-} and O_2^- anions, and result in an increase in the solubilities of the oxides and superoxides. This would lead to the acceleration of the oxygen-reduction reaction (ORR). Similar test results were obtained for a system with an electrolyte free of propylene carbonate (not shown here).

Handling of sodium metal and fabrication of the cell took place under an argon atmosphere in a vacuum glove box containing less than 10 ppm water. Following this, the cell was removed from the glove box, kept under nitrogen, placed in an oven and dry oxygen was passed over the air electrode at 10 mL min^{-1}. The operating temperature was 105–110 °C, just above the melting point of sodium (97.8 °C). The cells were tested with an Arbin model BT4 battery tester.

In order to prove that molten sodium can be cycled, we ran deposition–dissolution tests of sodium on aluminum at 105 °C, with the use of a 2032 coin cell. The electrolyte consisted of NaTf (NaCF$_3$SO$_3$, Aldrich reagent grade), Al_2O_3 (Degussa Ltd.), methyl methanesulfonate (Aldrich reagent grade) and PEO (5 × 10^6 MW, Aldrich reagent grade). NaTf and PEO were dried under vacuum at 150 °C, and 50 °C, respectively, for 48 h prior to use. Acetonitrile (ACN) (Aldrich battery grade, 99.93%, water content below 50 ppm), was used as solvent.

NaTf was dissolved in ACN at room temperature inside a sealed flask, and then PEO was added. The solution was carefully stirred in order to completely dissolve the PEO to form NaTf:P(EO)$_6$. The nanoporous Al_2O_3 powder (5% (w/w)) was vacuum-dried at 150 °C for 48 h and added to the solution. Methyl methanesulfonate, 5% (w/w), was also added to the slurry as an SEI precursor. The solution was then magnetically stirred at room temperature for 24 h to obtain a homogeneous slurry. The slurry was cast on a glass separator (150 μm) and the solvents were slowly removed (24 h) by room-temperature evaporation in an argon-atmosphere dry-box. Finally, the membranes were dried under vacuum at 50 °C for at least 24 h. The Na/NaTf:P(EO)$_6$ + 5% (w/w) methyl methane-sulfonate + 5% (w/w) Al_2O_3/Al cell was built in a 2032 coin-cell configuration. Cycle-life tests were conducted with the use of a Maccor battery cycler at a temperature of 105 °C for different electrodeposition/electrodissolution currents and times of operation. The cell was allowed to rest for 1–5 min between steps.

The impedance of the cells at 105 °C was determined by electrochemical-impedance spectroscopy. The measurements were conducted with the use of a Solartron 1255 Impedance Analyzer over the frequency range of 10 MHz–1 mHz. The coin cells were thermally equilibrated for at least 2 h at the operating temperature of 105 °C before the beginning of measurements.

3. Results and discussion

A scheme of a proposed sodium-air-battery stack is depicted in Fig. 2. The power generated by the sodium-air stack is determined by the number of cells integrated in the stack and their active area. The cells are connected in series in order to reach a specific voltage output. Typical single-cell thickness is estimated to be about 2 mm (Fig. 2). Light and low-cost hardware materials such as aluminum, that are compatible with oxygen and sodium (do not form alloys with sodium) can be used as thin bipolar plates.

A preliminary evaluation of energy- and power-density constraints was run for a lithium-air battery based on bipolar-plate
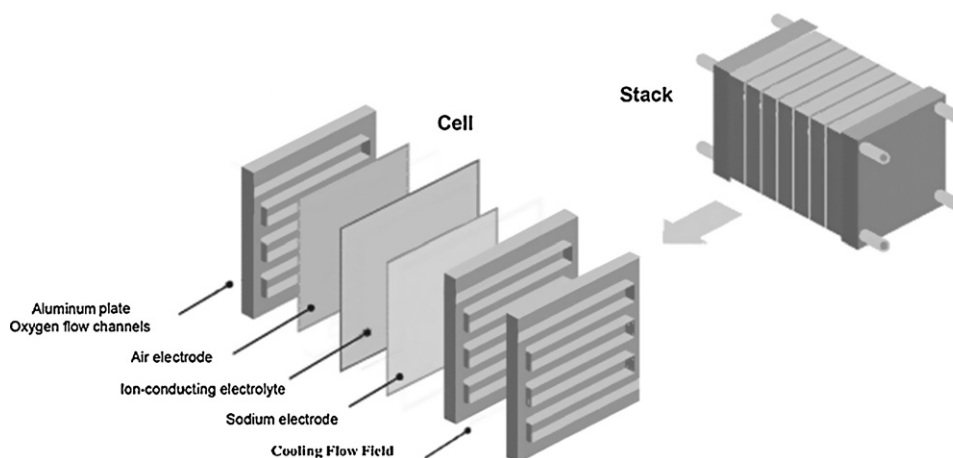
Fig. 2. Schematic structure of sodium/air single cell and stack. Each single cell consists of aluminum bipolar plates which contain the oxygen-flow channels, sodium electrode and air electrode with an ion-conducting matrix (electrolyte) between them. An aluminum flow-channel plate is added for the flow of a cooling fluid, for controlling temperature of the stack.

(BPP) design (similar to that shown in Fig. 2): for a 100 L, 100 kWh, 100 kW stack, $1 W mL^{-1}$ and $1 Wh mL^{-1}$ were obtained. For 2 mm-thick cells (vs. 0.2 mm in Li-ion batteries), at 2.5 V, the current and charge densities are $80 mA cm^{-2}$ and $80 mAh cm^{-2}$. If $1 Ah g^{-1}$ of carbon is assumed, $80 mg carbon cm^{-2}$ and about 0.8 mm-thick pristine-carbon electrode are obtained. For a 50 L stack (a volume similar to that of the Honda FCX Clarity FC stack (57 L)), $160 mA cm^{-2}$ and $160 mAh cm^{-2}$ and about 1.6 mm-thick pristine-carbon electrode are obtained. Thus it is concluded that due to the use of a thick air electrode, the lithium-air battery, based on BPP design, must run at about $0.1 A cm^{-2}$ in order to have practical volume and weight.

Sodium is much cheaper and more abundant than lithium. The theoretical specific energy of the sodium-air cell, on the assumption that Na_2O is the discharge product and including the weight of oxygen, is $1690 Wh kg^{-1}$ (it is $2271 Wh kg^{-1}$ excluding the oxygen weight), about four times that of state-of-the-art lithium-ion batteries. Since O_2 is not carried in the battery, values should be given as the average of the charge and discharge states. The battery weight will increase once discharge begins, hence the theoretical energy calculation should include O_2 in the discharged state and exclude O_2 in the fully charged state. Accordingly, the average specific energy density of the Na/O_2 cell is $1980 Wh kg^{-1}$. The open-circuit voltage of the sodium–oxygen cell is 2.3 V (for Na_2O_2 as the product) and 1.95 V (for Na_2O as the product ($\Delta G_f = -105 kcal mol^{-1}$ for Na_2O_2 and $\Delta G_f = -90 kcal mol^{-1}$ for Na_2O). These values are lower than that for the lithium-oxygen cell (3.1 V). We believe that if development is successful, the sodium-air battery could increase the driving range of an EV by a factor of four for the same battery weight of the lithium-ion battery.

We suggest here, for the first time, that the sodium-air battery be run at above the melting point of sodium. The surface tension of the liquid anode is expected to prevent the formation of dendrites on charge. Any sodium dendrites that might be formed would be absorbed into the liquid phase. The higher operating temperature accelerates electrode kinetics and reduces electrolyte resistance, thus enabling running the cell at higher power. Sodium peroxide is less stable and more reactive than lithium peroxide [14] and can be decomposed by a manganese dioxide catalyst (no such information is available for lithium peroxide). At the higher operating temperature and with the use of a proper four-electron ORR catalyst it may be possible to reduce oxygen to oxide (as Na_2O), thus avoiding the accumulation of peroxide in the air electrode. In contrast to lithium, sodium does not dissolve in aluminum (0.003%) [15], and this enables the use of aluminum as a light and low-cost hard-

ware material, especially for thin bipolar plates. By contrast, lithium cells require the use of copper or nickel as anode current-collector materials, both of them heavier and much more expensive than aluminum. At temperatures above 100 °C, the adsorption of water vapor by the cell components is negligible (most battery materials are dried at 100–150 °C). Thus, for operation at above 100 °C, less interference of atmospheric water is expected. In addition, unlike lithium, sodium does not form a nitride in air. In order to eliminate or reduce vibration of the molten sodium anode, that might adversely affect the SEI, it is preferred to absorb it into a porous matrix or a dense grid.

In order to create a protective SEI on alkali-metal anodes, it is essential that the equivalent volumes of the SEI materials be larger than that of the anode [16].

Only in this way, can the SEI cover the anode surface completely and stop corrosion. If not, the anode will continue to corrode. The equivalent volumes of Na_2CO_3, NaF and Na_2O are 20.87, 16 and 13.7 mL, respectively, all lower than that of sodium (23.7 mL). Thus these cannot serve as good SEI-building materials.

On the other hand, the equivalent volumes of several sodium oxosulfur compounds including $Na_2S_2O_4$, $Na_2S_2O_3$ and Na_2SO_4 are 39.7, 47.4 and 26.7 mL, respectively, which makes them suitable candidates for use as sodium-SEI-building materials. Another possible solution is the use of a preformed artificial SEI [17]. Fig. 3 represents the discharge/charge curves of the fourth cycle of a molten-Na/O_2 cell in the 1.5–3.0 V voltage range (or 20 min operation time) at 105 °C. The discharge and charge currents were 50 μA and 100 μA, respectively. The cell was allowed to rest between discharge and charge for 1 min. As can be seen from this graph, a voltage plateau of 1.75 V was obtained on discharge and one close to 3 V on charge. At rest, the OCV was close to 2 V.

In Fig. 4, the discharge/charge curves of the fifth cycle are shown for the same cell and operating parameters as in Fig. 3. When the oxygen supply was stopped, the cell voltage immediately dropped to 1.5 V, thus proving that oxygen was the active cathode material. The oxygen supply was then reactivated, and cell voltage return to the normal value of 1.75 V.

The deposition–dissolution process of molten sodium on aluminum was studied at 105 °C. A $1.8 cm^2$ solid-polymer-electrolyte disc was sandwiched between an aluminum foil and a $0.57 cm^2$ sodium–metal disc, and hermetically sealed in a 2032 coin cell. The assembly of the cell was carried out in an argon-atmosphere dry-box with humidity content below 10 ppm. Fig. 5 shows the variation of cell potential with time. The sodium-dissolution process was stopped at a cell voltage of 1.5 V. After cell discharge
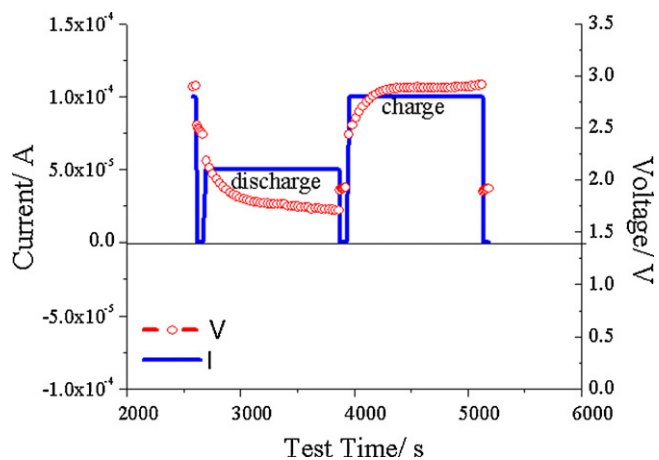
Fig. 3. Discharge/charge curves of a Na/O$_2$ cell at 105 °C, 1.5–3.0 V (or 20-min operating time), discharge and charge currents are 50 μA and 100 μA, respectively. (FC hardware, electrode area—1 cm^2, ETEK cathode). The electrolyte consists of 0.1 M CP, 1 M NaClO$_4$ and 1% (w/w) Al$_2$O$_3$ nano-powder dispersed in PEGDME 2000 and propylene carbonate (PC) (90:10).
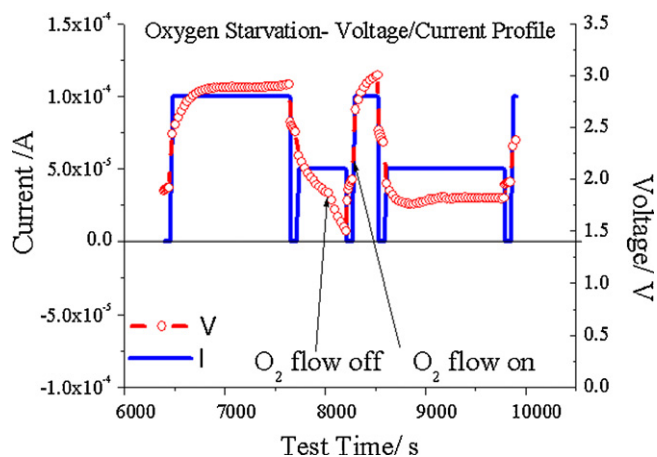
Fig. 4. Oxygen-starvation test of a Na/O$_2$ cell described in Fig. 3 at 105 °C.
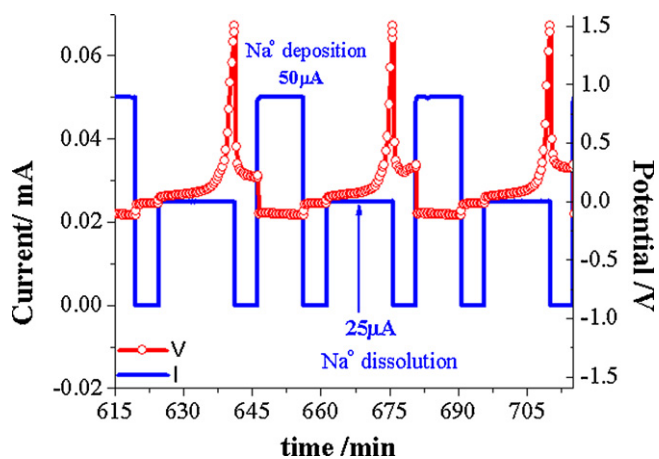
Fig. 5. Sodium deposition–dissolution on Al at 105 °C. Na/NaTf:P(EO)$_6$ + 5% (w/w) methyl methanesulfonate + 5% (w/w) Al$_2$O$_3$/Al cell. Discharge and charge rates are 50 μA for 10 min and 25 μA for 20 min, respectively. Coin-cell hardware. Electrode area −0.57 cm^2.
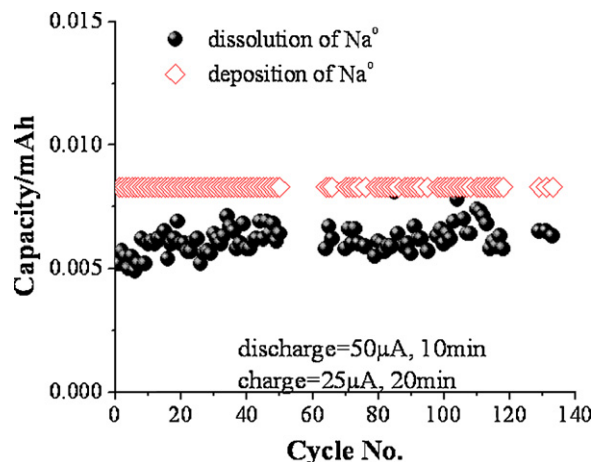
Fig. 6. Deposition and dissolution cycles of Na on Al at 105 °C, cell described in Fig. 5.

(sodium plating on aluminum), the measured OCV was a few millivolts, a clear indication of plating of sodium on the aluminum electrode. The cell voltage measured during sodium dissolution at 25 μA and at half of the dissolution time was 0.1 V, while the cell voltage measured during sodium deposition at 50 μA at half of the deposition time was 0.07 V. Thus, a value of 1596 Ω cm^2 can be calculated for the cell resistance during sodium dissolution from aluminum, and 1140 Ω cm^2 during sodium plating on aluminum. This cell resistance is the sum of three resistors: the sodium–metal-SEI resistor, the electrolyte resistor and the resistor of the SEI on sodium that was deposited on aluminum. The larger portion of the cell resistance is assigned to the sum of the two SEI resistors as we show in Fig. 7. The cell voltage, during these constant-current tests, rose with the number of the deposition–dissolution cycles.

Fig. 6 shows the cycle life of a Na/NaTf:P(EO)$_6$ + 5% (w/w) methyl methanesulfonate + 5% (w/w) Al$_2$O$_3$/Al cell at 105 °C. Successive cycling was conducted at a discharge (deposition) and charge (dissolution) rate of 50 μA for 10 min and 25 μA for 20 min, respectively. We succeeded in cycling this molten-sodium cell for over 140 cycles, without the appearance of dendrites. The faradaic efficiency of the deposition/dissolution process (sodium-dissolution charge divided by sodium-deposition charge) of molten sodium was about 85% at the 100th cycle. It is lower than what is necessary (over 99% efficiency) for a good rechargeable sodium battery; however, since what is presented here is the first attempt at depositing sodium in its liquid state, it is a good starting point.

In lithium and lithium ion batteries the anode is covered by a solid electrolyte interphase (SEI) [9–11]. The typical capacitance of the anode SEI in these batteries is in the range 10^{-6}–10^{-7} μF cm^{-2} and it is associates with a 10–100 nm thick SEI [9–11]. Fig. 7 shows the AC-impedance spectra at 105 °C of the same cell as described in Fig. 5, measured after the plating of sodium on aluminum. As can be seen from Fig. 7, the bulk (electrolyte) resistance is about 60 Ω and there are two different semi-circles in the SEI-frequency regions. These two SEIs are assigned to two different interphases of sodium and the electrolyte. The first is ascribed to the interphase between the original sodium foil and the electrolyte, and the latter to the interphase between the sodium-plated aluminum and the electrolyte. The resistance of both SEIs, 308 and 353 Ω cm^2, respectively, are similar to those measured for the lithium anode in nonaqueous solutions [9–11]. The capacitances of these two SEIs are 0.2 and 1.7 μF, from which the SEI thickness is calculated to be 252 and 30 Å, respectively. These values of the SEI thickness are very similar to those measured for lithium metal in nonaqueous solutions [9–11]. The ionic conductivity of the electrolyte, calculated
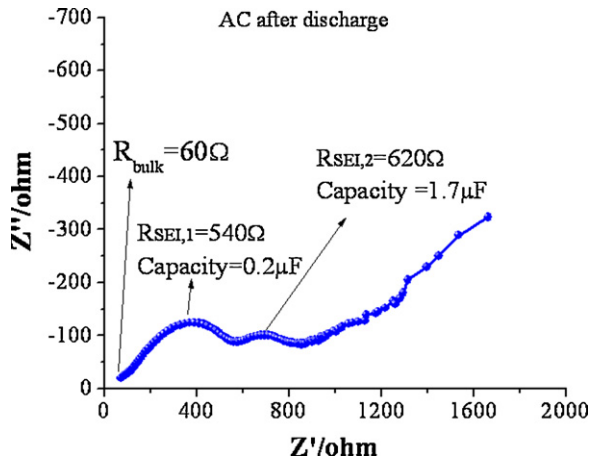
Fig. 7. AC-impedance spectra of Na/NaTf:P(EO)$_6$ + 5% (w/w) methyl methanesulfonate + 5% (w/w) Al$_2$O$_3$/Al cell at 105 °C, after plating of Na on Al, frequency range—10 MHz to 1 mHz. Electrode area –0.57 cm^2.

from the bulk resistance at 105 °C is 0.5 mS cm^{-1}, a value similar to that measured for Li$^+$-conducting polymer electrolytes at about 100 °C [18].

Fig. 8 schematically presents the reaction mechanisms for oxygen reduction and oxide (or peroxide) oxidation on the surface of the cathode at the end of discharge when the cathode surface is completely covered by a thin layer of oxide and peroxide particles. The air electrode (Fig. 8a) in an alkali-metal/air battery must be composed of three phase regions similar to those of the air electrode in a PEM fuel cell. To each catalyst nanoparticle at the cathode, electrons must flow from the cathode current collector, and oxygen must arrive from the air-flow field and diffuse through the thin electrolyte film covering the catalyst nanoparticle. The alkali-metal cations must move from the anode through the electrolyte. When an alkali-metal/air cell begins to discharge, peroxide particles deposit on the surface of the cathode. Electrons tunnel through this thin peroxide layer and continue to react with oxygen molecules and alkali-metal cations (Fig. 8b) at the oxide/electrolyte interface until its thickness is too great to enable further electron tunneling (estimated at about 25 Å). At this point, the battery impedance is too high and the cell cannot deliver power—in other words, its capacity is exhausted. This process is similar to the formation of a fresh SEI when lithium metal is immersed in a battery electrolyte [9–11]. At the carbon(or catalyst)/peroxide interface, especially at low operating cell voltage, the peroxide can be further reduced to oxide. So it is expected that a double-layer passivating film will be formed, the layer next to the carbon consisting mainly of oxide particles and that next to the electrolyte consisting mainly of peroxide particles. On charge, the oxidation of the oxide/peroxide particles can proceed in two ways. According to option A (Fig. 8c), electrons tunnel from the peroxide/electrolyte interface to the carbon (or catalyst) surface, releasing alkali-metal cations and oxygen molecules. According to option B (Fig. 8d) the electron-transfer reaction takes place at the catalyst/oxide interface, releasing alkali-metal cations and oxygen molecules which cross the thin oxide/peroxide layer into the electrolyte. In this path, the pressure of oxygen gas can increase, causing a break in the film, a process which may easily further promote film oxidation, on the one hand and, on the other, cause a loss of connection of oxide particles to the electrode. The real processes are probably much more complex and we present here just a simple case. On the assumption that the final product is oxide and the tunneling range of electrons through the oxide layer is 25 Å, it is possible to calculate the maximum charge per surface area of carbon (in terms of Ah cm^{-2}) and the capacity per gram of carbon. The result obtained for carbon with
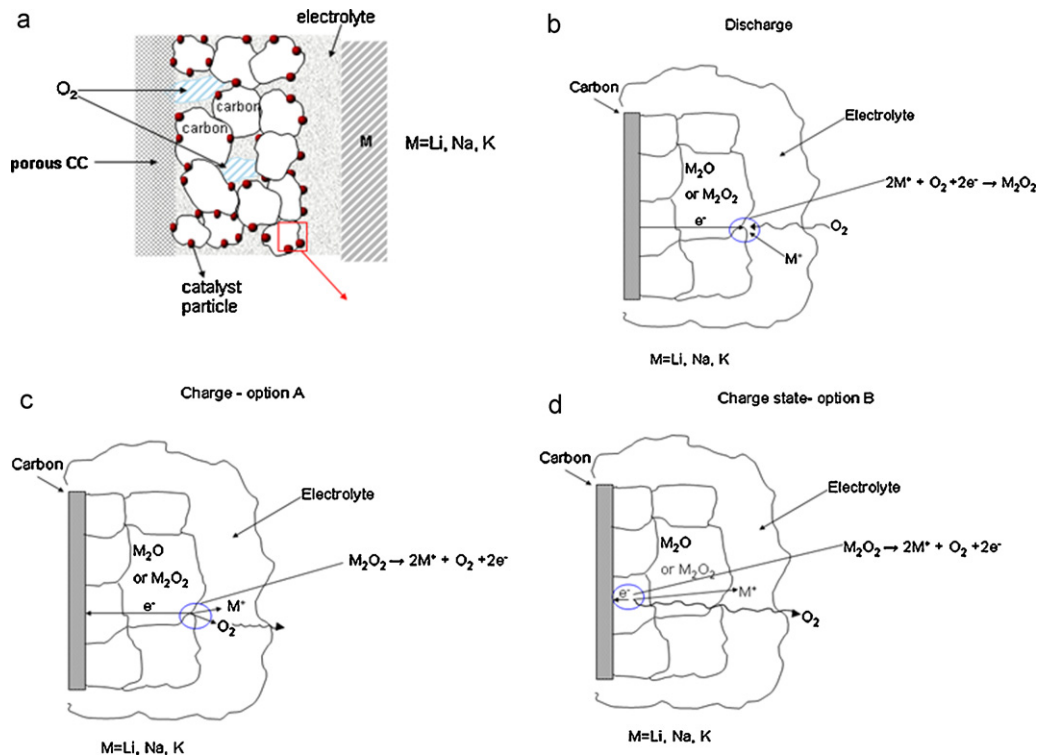
Fig. 8. Schematic description of oxygen-reduction and oxide-oxidation mechanisms on the cathode surface of an alkali-metal/air cell. (a) Three phase regions of the air electrode (oxygen, electrolyte and catalyst). (b) Deposition of peroxide (or oxide) particles during discharge. (c) On charge, alkali-metal cations and oxygen molecules are released while electrons tunnel through the thin oxide/peroxide layer (option A) or, (d) The released alkali-metal cations and oxygen molecules cross the thin oxide/peroxide layer (option B).

an available surface area of $200\,\mathrm{m^2\,g^{-1}}$, is a maximum capacity of $1\,\mathrm{Ah\,g^{-1}}$.

4. Conclusions

The necessary conditions for success in the development of practical, safe, smaller and lower-cost lithium and sodium-air rechargeable EV batteries are as following: elimination of the formation of dendritic deposits (on charge); increasing the current density up to $100\,\mathrm{mA\,cm^{-2}}$ (or reduction of cell DC resistance to less than $10\,\Omega\,\mathrm{cm^2}$); and change the oxygen-discharge product from peroxide to oxide.

In this paper we demonstrated only 85% faradaic efficiency for sodium deposition/dissolution at temperatures higher than $100\,^\circ\mathrm{C}$. Increase of the faradaic efficiency to above 99.5% is crucial. We have found that the thickness and resistance of the sodium SEI at $100\,^\circ\mathrm{C}$ are similar to the values measured for lithium in lithium batteries at room temperature. A model explaining the mechanism of oxygen reduction and oxide oxidation is presented.

We would like to emphasize that the use of a liquid sodium anode at above $100\,^\circ\mathrm{C}$ may solve or alleviate several problems, including: acceleration of sluggish cathode reactions and lowering of the cell impedance, elimination of dendrites formation, minimization of interference by water vapor and CO_2, and utilization of, lighter and lower-cost hardware materials like aluminum.

References

[1] K.M. Abraham, Z. Jiang, J. Electrochem. Soc. 143 (1996) 1.
[2] P.G. Bruce, J. Am. Chem. Soc. 128 (2006) 1390–1393.
[3] A. Deĭbart, A.J. Paterson, J. Bao, P.G. Bruce, Angew. Chem. Int. Ed. 47 (2008) 4521.
[4] B. Kumar, J. Kumar, R. Leese, J.P. Fellner, S.J. Rodrigues, K.M. Abraham, J. Electrochem. Soc. 157 (1) (2010) A50–A54.
[5] G. Girishkumar, B. McCloskey, A.C. Luntz, S. Swanson, W. Wilcke, J. Phys. Chem. Lett. 1 (2010) 2193–2203.
[6] T. Zhang, N. Imanishi, Y. Shimonishi, A. Hirano, Y. Takeda, O. Yamamoto, N. Sammes, Chem. Commun. 46 (2010) 1661–1663.
[7] C.O. Laoire, S. Mukerjee, K.M. Abraham, J. Phys. Chem. 113 (2009) 20127–20134.
[8] E. Peled, Parameter analysis of a practical lithium- and sodium-air ev battery, http://www.tau.ac.il/institutes/ifcbc/presentations-2010.html/.
[9] E. Peled, in: J.P. Gabano (Ed.), Lithium Batteries, Academic Press, 1983, p. 43.
[10] E. Peled, J. Electrochem. Soc. 126 (1979) 2047.
[11] E. Peled, D. Golodnitsky, in: P. Balbuena, Y. Wang (Eds.), Lithium-Ion Batteries: Solid-Electrolyte Interphase, Imperial College Press, 2004.
[12] A. Blum, T. Duvdevani, M. Philosoph, N. Rudy, E. Peled, J. Power Sources 5449 (2003) 1–4.
[13] D. Golodnitsky, R. Kovarsky, H. Mazor, Yu. Rosenberg, I. Lapides, E. Peled, W. Wieczorek, A. Plewa, M. Siekierski, M. Kalita, L. Settimi, B. Scrosati, L.G. Scanlon, J. Electrochem. Soc. 154 (6) (2007) A547–A553.
[14] ChemicalBook Copyright 2007 CAS NO: 1313-60-6, at: http://www.chemicalbook.com/.
[15] H. Baker (Ed.), ASM Handbook, vol. 3. Alloy Phase Diagrams, ASM International, 1992.
[16] E. Peled, D. Golodnitsky, C. Menachem, D. Bar-Tov, J. Electrochem. Soc. 145 (10) (1998) 3482–3486.
[17] S. Menkin, D. Golodnitsky, E. Peled, Electrochem. Commun. 11 (2009) 1789–1791.
[18] F.M. Gray, Solid Polymer Electrolytes: Fundamentals and Technological Applications, VCH Publishers, New York, 1991.